

## Nuclear Magnetic Resonance in Hexagonal Lanthanum Metal: Knight Shifts, Spin Relaxation Rates, and Quadrupole Coupling Constants\*

ALBERT NARATH

*Sandia Laboratories, Albuquerque, New Mexico 87115*

(Received 14 November 1968)

The  $^{139}\text{La}$  nuclear magnetic resonances in the double-hexagonal close-packed (dhcp) form of metallic lanthanum have been studied by spin-echo techniques in the frequency range 6–30 MHz and temperatures between  $\sim 1$  and 210°K. A seven-line powder pattern due to electric quadrupole interactions is observed with  $|e^2qQ(^{139}\text{La})/h^{-1}| = 7.8 \pm 0.3$  MHz. The quadrupole splittings are identical within the experimental uncertainty for the two crystallographic sites. The Knight shifts are very different, however,  $K \approx +0.63\%$  and  $+1.02\%$  at 4°K, and  $K \approx +0.59\%$  and  $+0.92\%$  at 210°K. The anisotropic Knight-shift contribution is estimated to be less than 10% of the measured shifts. The average spin-lattice relaxation time for the two sites is  $T_1T = 0.56 \pm 0.05$  sec °K. The relaxation time for the site having the smaller Knight shift exceeds that for the other site by a factor of approximately 1.7. A comparison of the average Knight shifts and spin-lattice relaxation rates in dhcp lanthanum with those in hcp scandium and yttrium leads to the conclusion that the direct *s*-contact interaction is the dominant magnetic-hyperfine mechanism in the Group-IIIB transition metals.

### I. INTRODUCTION

AS part of a continuing investigation of nuclear magnetic resonance (NMR) in the hexagonal Group-IIIB and -IVB transition metals we have studied the  $^{139}\text{La}$  NMR in lanthanum metal by spin-echo techniques.<sup>1</sup> The long-range aim of this program is to elucidate the origins of the observed hyperfine interactions in these metals. Of particular interest is the influence of many-body effects on the Knight shifts and spin-lattice relaxation rates.

Lanthanum ( $5d^16s^2$ ) is the heaviest of the Group-IIIB transition elements. This group also includes scandium ( $3d^14s^2$ ) and yttrium ( $4d^15s^2$ ). [Lutetium ( $4f^{14}5d^16s^2$ ) should probably also be included in this list because of its close resemblance to scandium and yttrium.] The elemental Group-IIIB metals are characterized by large electronic specific heats<sup>2,3</sup> and temperature-dependent magnetic susceptibilities.<sup>4</sup> In this respect they resemble the Group-VIII metals nickel, palladium, and platinum which terminate the respective transition series. The platinum-group transition metals are distinguished by spin susceptibilities which are strongly enhanced over their independent electron values by repulsive electron-electron interactions. The exchange enhancement is strongest in nickel and decreases, as expected, with increasing atomic number. Among the Group-IIIB metals, strong exchange enhancement effects have been clearly identified in the

case of scandium.<sup>5</sup> Moreover, the progressive decrease in the observed susceptibilities in the sequence scandium to lanthanum, when contrasted with the nearly constant electronic specific-heat coefficients, is again consistent with a reduction in the magnitude of the exchange enhancement for the heavier members of the group. In addition to the electron-electron interactions, electron-phonon effects are also of importance in the Group-IIIB metals.<sup>6</sup> These are particularly evident in the case of lanthanum, whose Debye temperature ( $\Theta_D = 142^\circ\text{K}$ ) is considerably lower than would have been expected from an interpolation of the linear  $\Theta_D^2$  versus atomic-mass variation for the other hexagonal Group-IIIB and -IVB transition metals.<sup>7,8</sup>

Lanthanum crystallizes in two allotropic forms.<sup>9</sup> At high temperatures the stable modification is the face-centered-cubic (fcc) structure which corresponds to an *ABC* stacking sequence of close-packed atomic layers. Below  $\sim 260^\circ\text{C}$  a transformation to the double-hexagonal close-packed (dhcp) structure occurs. The dhcp structure differs from the more common hcp structure of scandium and yttrium in that the stacking sequence is *ABAC* instead of *ABAB*. This results in a doubling of the *c*-axis lattice constant and thus an "ideal" *c/a* ratio of  $2 \times (8/3)^{1/2} = 3.2650$ . It follows that the dhcp structure, with four atoms per unit cell, contains two nonequivalent sites: The *A*-layer sites are characterized by cubic nearest-neighbor coordination when the *c/a* ratio has the ideal value, while the *B*- and *C*-layer sites are characterized by hexagonal nearest-neighbor coordination. With a *c/a* ratio of 3.2252, lanthanum

\* This work was supported by the U. S. Atomic Energy Commission.

<sup>1</sup> A preliminary account of this work appeared in *Bull. Am. Phys. Soc.* **13**, 473 (1968).

<sup>2</sup> H. Montgomery and G. P. Pells, *Proc. Phys. Soc. (London)* **78**, 622 (1961).

<sup>3</sup> A. Berman, M. W. Zemansky, and H. A. Boorse, *Phys. Rev.* **109**, 70 (1958).

<sup>4</sup> For the most recent experimental results and complete references to earlier work, see D. K. Wohlleben, thesis, University of California, San Diego, 1968 (to be published).

<sup>5</sup> W. E. Gardner and J. Penfold, *Phil. Mag.* **11**, 549 (1964).

<sup>6</sup> See, for example, A. M. Clogston, *Phys. Rev.* **136**, A8 (1964).

<sup>7</sup> T. Kasuya, in *Magnetism*, edited by G. T. Rado and H. Suhl (Academic Press Inc., New York, 1966), Vol. 2B, Chap. 3.

<sup>8</sup> M. A. Jensen, in *Proceedings of the NATO Advanced Summer Study Institute on Superconductivity* (Gordon and Breach, Science Publishers, Inc., New York, 1968).

<sup>9</sup> F. H. Spedding, A. H. Daane, and K. W. Herrmann, *Acta Cryst.* **9**, 559 (1956).

approximates the ideal dhcp structure, and thus affords the opportunity to examine the sensitivity of the magnetic-hyperfine interactions on the local site symmetry. Furthermore, since  $^{139}\text{La}$  ( $I = \frac{7}{2}$ ) has an electric quadrupole moment<sup>10</sup> ( $Q \approx 0.21 b$ ), it is in principle possible by means of NMR experiments to detect differences between the electric field gradients at the two nonequivalent crystallographic sites.

The first observation of NMR in lanthanum metal was reported by Blumberg *et al.*,<sup>11</sup> who obtained essentially identical results for the cubic and hexagonal forms using steady-state techniques. A single, relatively narrow line was observed in both cases. The Knight shift was found to be temperature-dependent, increasing by approximately 15% on cooling from room temperature to 1.7°K. These authors also estimated the  $^{139}\text{La}$  spin-lattice relaxation rates from the low-temperature saturation behavior of the resonance. By means of transient techniques, Masuda<sup>12</sup> subsequently obtained relaxation rates for a lanthanum sample of unknown composition that were four times faster than those reported by Blumberg *et al.*<sup>11</sup> More recent experiments by Zamir and Schreiber<sup>13</sup> on fcc lanthanum support the findings of Blumberg *et al.*<sup>11</sup> The first evidence for large electric quadrupole interactions in dhcp lanthanum was provided by the NMR experiments of Torgeson and Barnes<sup>14</sup> who detected a three-line resonance spectrum in a powdered specimen in external fields near 25 kOe. These lines were assigned to the central transition and the innermost pair of satellites of the expected seven-line first-order quadrupole powder spectrum. The failure to observe the outer two pairs of satellite transitions was attributed to inhomogeneities in the electric field gradient arising from lattice strains or stacking faults. This interpretation led to the conclusion that the Knight shifts and quadrupole coupling constants were essentially identical for the two sites in the dhcp structure.

The present work was carried out on the dhcp form of lanthanum. The full seven-line quadrupole spectrum has been observed for the first time. It yields quadrupole coupling constants for the two sites whose magnitudes are experimentally indistinguishable although almost six times larger than those inferred by Torgeson and Barnes.<sup>14</sup> This discrepancy is shown to be the direct result of a large difference, previously undetected, between the Knight shifts at the two sites. Our experimental techniques are detailed in Sec. II of this paper. Results of measurements of the quadrupole coupling constants, Knight shifts, and relaxation rates are presented in Sec. III and discussed in Sec. IV. A summary of the principal conclusions is offered in Sec. V.

<sup>10</sup> K. Murakawa, *Phys. Rev.* **110**, 393 (1958).

<sup>11</sup> W. E. Blumberg, J. Eisinger, V. Jaccarino, and B. T. Matthias, *Phys. Rev. Letters* **5**, 52 (1960).

<sup>12</sup> Y. Masuda, *J. Phys. Soc. Japan* **19**, 239 (1964).

<sup>13</sup> D. Zamir and D. S. Schreiber, *Phys. Rev.* **136**, A1087 (1964).

<sup>14</sup> D. R. Torgeson and R. G. Barnes, *Phys. Rev.* **136**, A738 (1964).

## II. EXPERIMENTAL TECHNIQUES

Most of the experimental measurements were performed on 99.9% lanthanum metal obtained from the Research Chemicals Division of the Nuclear Corporation of America. In order to convert the specimen completely to the dhcp form it was vacuum annealed for about 72 h near 200°C. Preparation of 200 mesh powders was accomplished by means of a small milling machine using tungsten carbide cutters. During this operation the metal was submerged in Dow Corning 704 silicone fluid for protection from the atmosphere. The comminuted samples were usually reannealed and then mixed with a small amount of powdered KCl for electrical isolation. As a check on the reliability of the present results many of the experiments were repeated on the same sample used in the work of Torgeson and Barnes.<sup>14</sup> No significant differences were observed.

The NMR measurements were carried out in the frequency range 6–30 MHz with a phase-coherent crossed-coil transient spectrometer. Radio-frequency excitation was provided by a 15-kW gated amplifier. The receiver consisted of a tuned preamp, broadband rf amplifier, balanced mixer, video amplifier, and boxcar integrator.

Magnetic fields were produced by a compensated NbZr superconducting solenoid. A separate Dewar inserted into the magnet bore allowed a wide range of stable sample temperatures to be achieved by means of liquid helium, neon, nitrogen, and freon (R22).

Because of the inhomogeneous broadening of the resonances resulting from the strong electric quadrupole interactions, all measurements were made on spin echos produced by two equal-width rf pulses. Line profiles were obtained at fixed frequency by recording the variation of the integrated echo intensity as a function of external magnetic field strength. Knight shifts were calculated from the experimental frequency/field ratios using the reference ratio,  $\nu(\text{ref})/H = 0.60144$  kHz/Oe.<sup>15</sup> Spin-lattice relaxation rates were obtained from the recovery of the echo intensity following a saturating comb of closely spaced rf pulses. Echo phase-memory times were obtained from the decay of the nuclear signal with increasing time separation between the two rf pulses.

## III. EXPERIMENTAL RESULTS

### A. Nuclear Resonance Line Shapes

The naturally abundant isotope  $^{139}\text{La}$  has spin  $I = \frac{7}{2}$ . The first-order quadrupole spectrum<sup>16</sup> of lanthanum metal should therefore consist of six  $m \leftrightarrow m-1$  satellite transitions equally spaced about an undisplaced  $+\frac{1}{2} \leftrightarrow -\frac{1}{2}$  central transition. In a powder the observed satellite

<sup>15</sup> R. E. Sheriff and D. Williams, *Phys. Rev.* **82**, 651 (1951).

<sup>16</sup> For a review of nuclear electric quadrupole effects in solids, see M. H. Cohen and F. Reif, in *Solid State Physics*, edited by F. Seitz and D. Turnbull (Academic Press Inc., New York, 1957), Vol. 5.

resonances are broadened since the first-order splittings depend on the orientation of the external magnetic field. The positions of maximum resonance intensity, for the case of an axially symmetric electric field gradient, correspond to field shifts

$$\Delta H_m^{(1)} = (\pi/\gamma_n)(m - \frac{1}{2})\nu_Q, \quad (3.1)$$

where  $\gamma_n$  is the nuclear gyromagnetic ratio, and  $\nu_Q$  is defined in terms of the principal component  $q$  of the electric-field-gradient tensor and the nuclear electric quadrupole moment  $Q$ ,

$$\nu_Q = h^{-1}e^2qQ[3/2I(2I-1)]. \quad (3.2)$$

Figure 1 shows an example of a spin-echo spectrum for dhcp lanthanum at a fixed frequency of 11.89 MHz. Although the outermost pair of satellites is weak, the spectrum clearly exhibits the expected seven-line structure. Because of uncertainties inherent in the interpretation of spin-echo intensities, a detailed comparison of the experimental spectral shapes with theoretical predictions was not attempted. Quantitative significance was therefore attached only to the observed splittings. The spacing of the satellite lines yields

$$\nu_Q = 0.56(2) \text{ MHz}, \quad (3.3)$$

where the quantity in parentheses indicates the maximum estimated uncertainty in the preceding digit. The present value for  $\nu_Q$  is nearly six times larger than that of Torgeson and Barnes.<sup>14</sup> Their experimental observation of a closely spaced triplet at a frequency of 15.5 MHz suggests that this structure is associated only with the central transition. Such splitting could result from the combined effects of second-order quadrupole shifts of the central transition and a large difference between the Knight shifts at the two nonequivalent sites of the dhcp structure. In a powdered specimen the second-order quadrupole effects produce a central-

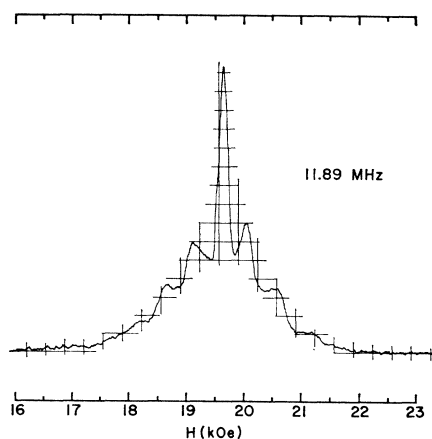


FIG. 1. Spin-echo spectrum of  $^{139}\text{La}$  in dhcp lanthanum metal at a constant frequency of 11.89 MHz and  $T = 1.2^\circ\text{K}$ . The spectrum was obtained with two 30- $\mu\text{sec}$ -wide rf pulses separated by 50  $\mu\text{sec}$ .

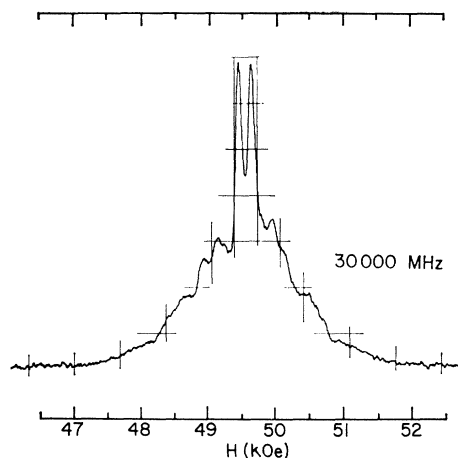


FIG. 2. Spin-echo spectrum of  $^{139}\text{La}$  in dhcp lanthanum metal at 30.000 MHz. Other experimental conditions were the same as for the 11.89-MHz spectrum in Fig. 1.

transition splitting, at a constant frequency  $\nu_0$ , which for  $I = \frac{7}{2}$  is given by

$$\begin{aligned} \Delta H_{1/2}^{(2)} &= (\pi/\gamma_n) \{ [\nu_0^2 + (20/3)\nu_Q^2]^{1/2} \\ &\quad - [\nu_0^2 - (15/4)\nu_Q^2]^{1/2} \} \\ &\approx (\pi/\gamma_n) [125\nu_Q^2(24\nu_0)^{-1}]. \end{aligned} \quad (3.4)$$

For  $\nu_0 = 15.5$  MHz and  $\nu_Q = 0.56$  MHz, Eq. (3.4) predicts a splitting of 87 Oe, which corresponds to  $\sim 0.34\%$  of the applied field. Thus, a Knight-shift difference of approximately the same magnitude would produce the triplet pattern observed by Torgeson and Barnes. Other explanations, such as possible interference from fcc lanthanum, were eliminated by studies of the frequency dependence of the spectral shape. As expected, the spectrum gradually transforms with increasing frequency into two identical seven-line first-order quadrupole patterns with a relative displacement of 0.4%. This is demonstrated by the 30 MHz spectrum in Fig. 2. At this frequency the second-order splitting has decreased to 45 Oe (i.e., 0.09%), and the shape of the spin-echo spectrum is consequently dominated by the Knight-shift difference. The change from low-field to high-field behavior is illustrated by the central-transition spectra in Fig. 3. At 6.2 MHz [Fig. 3(a)] the second-order quadrupole splitting (2.1%) is much larger than the differential Knight shift, and the observed powder spectrum approximates a doublet structure. At 15.5 MHz [Fig. 3(b)] the two effects have nearly equal magnitude and yield a partially resolved triplet structure. Finally, at 30.0 MHz [Fig. 3(c)] the differential Knight shift has become dominant, resulting in a well-resolved doublet structure.

In contrast to the Knight shifts, the quadrupole coupling constants at the two sites appear to be essentially identical in magnitude. This conclusion is based on two observations: (1) Three satellite pairs are clearly resolved at low frequencies. A large differ-

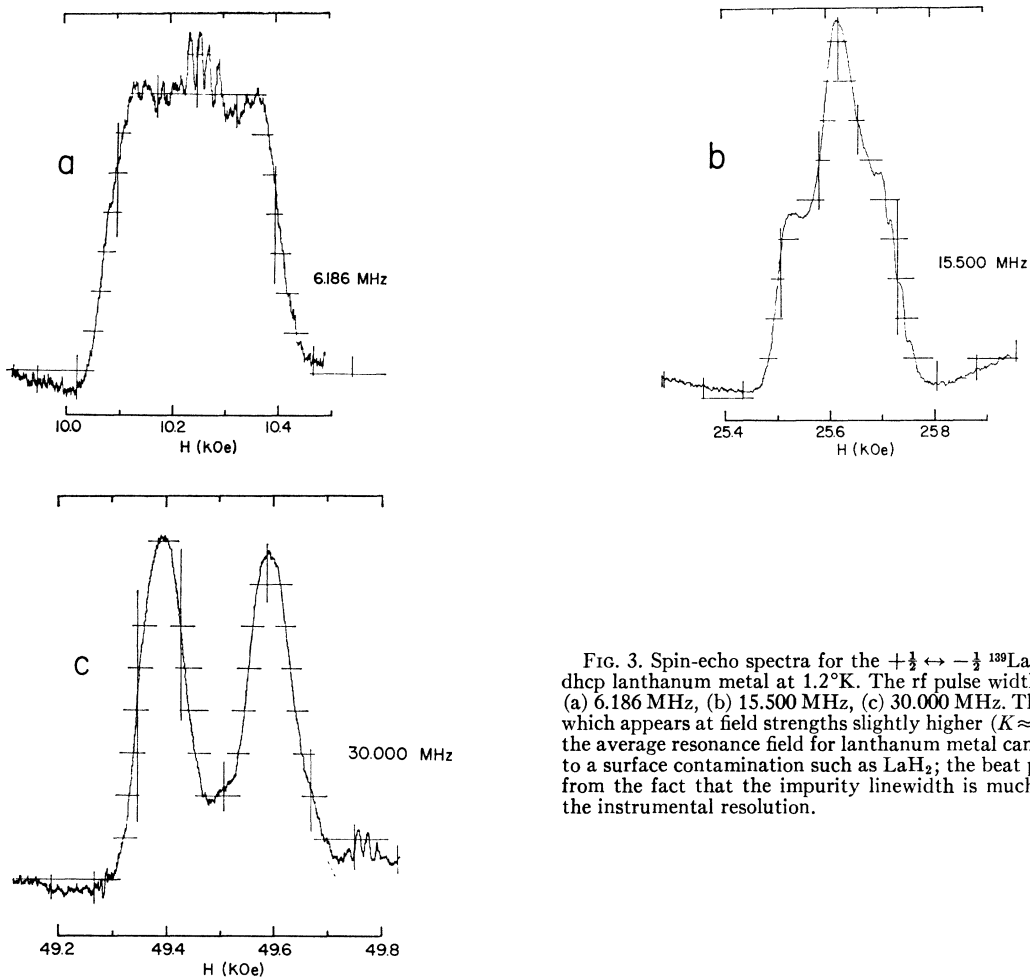


FIG. 3. Spin-echo spectra for the  $+\frac{1}{2} \leftrightarrow -\frac{1}{2}$   $^{139}\text{La}$  transitions in dhcp lanthanum metal at 1.2°K. The rf pulse width was 50  $\mu\text{sec}$ , (a) 6.186 MHz, (b) 15.500 MHz, (c) 30.000 MHz. The interference which appears at field strengths slightly higher ( $K \approx +0.2\%$ ) than the average resonance field for lanthanum metal can be attributed to a surface contamination such as  $\text{LaH}_2$ ; the beat pattern results from the fact that the impurity linewidth is much smaller than the instrumental resolution.

ence in the two coupling constants would either double the number of observed lines, or more likely, would wash out the satellite structure. (2) The partially resolved Knight-shift splitting of the satellite lines at high frequencies yields independent estimates for both coupling constants which again are indistinguishable. These results indicate that the coupling constants differ by at most 10%. The possibility that one of the coupling constants is very much smaller than the other can be rejected because of the observation of two equal intensity  $+\frac{1}{2} \leftrightarrow -\frac{1}{2}$  lines at high frequencies.

TABLE I. Summary of Knight-shift measurements for the high-field  $K(1)$  and low-field  $K(2)$   $^{139}\text{La}$  nuclear resonances in dhcp lanthanum metal.

$T$ (°K)	$K(1)$ (%)	$K(2)$ (%)
4	+0.63(5)	+1.02(5)
27	+0.62(5)	+1.02(5)
76	+0.64(5)	+1.01(5)
144	+0.60(5)	+0.94(5)
210	+0.59(5)	+0.92(5)

At sufficiently high frequencies the positions of maximum intensity of the two central transitions yield Knight shifts ( $K$ ) which, because of the noncubic site symmetries, are composed of isotropic ( $K_{\text{iso}}$ ) and anisotropic ( $K_{\text{ax}}$ ) contributions.<sup>17</sup> A summary of the experimental values of  $K$  as a function of temperature is given in Table I. The shifts were measured at 30 MHz where second-order quadrupole shifts of the peak positions of the resonance are comparable in magnitude to the experimental errors and can therefore be neglected. It is worthwhile to note that the observed temperature dependence of the shifts in dhcp lanthanum is identical within the combined experimental uncertainties to that in fcc lanthanum.<sup>11</sup> Furthermore, the average dhcp shift (0.83%) at 4°K has essentially the same magnitude as the fcc shift (0.76%).<sup>11</sup>

In principle, the separation of  $K$  into isotropic and anisotropic terms can be accomplished even in a powder specimen by measuring the dependence of the central-transition line width on  $\nu_0$ , since the broadening due to

<sup>17</sup> See, for example, W. H. Jones, Jr., T. P. Graham, and R. G. Barnes, Phys. Rev. **132**, 1898 (1963).

second-order quadrupole effects varies as  $\nu_0^{-1}$ , while that due to Knight-shift anisotropy varies as  $\nu_0$ . In the present case  $\nu_Q$  is too large to make this procedure feasible with the maximum field strength of  $\sim 60$  kOe available to us (i.e., the shape of the central transition is dominated by the anisotropic Knight shift only when  $\nu_0 > 30$  MHz). The magnitude of  $K_{ax}$  can nevertheless be estimated by noting that the half-intensity widths of both central transitions at 30 MHz are  $\sim 0.19\%$ , or approximately twice the value expected from second-order quadrupole effects alone. An upper-limit estimate for  $K_{ax}$  can therefore be obtained by attributing the excess linewidths entirely to Knight-shift anisotropies, i.e., by neglecting the effects of dipolar broadening and inhomogeneities in the isotropic Knight shift. With the additional assumption that  $K_{ax} < 0$  as in scandium and yttrium metals,<sup>18</sup> the central-transition widths (for  $I = \frac{7}{2}$  and parameter values appropriate to the present case) are then given approximately by<sup>17</sup>

$$\Delta H_{1/2} = (2\pi/\gamma_n) [(125/48)\nu_Q^2\nu_0^{-1} - (5/3)K_{ax}\nu_0 + (4/15)K_{ax}^2\nu_0^3\nu_Q^{-2}]. \quad (3.5)$$

Substitution of the measured values of  $\nu_Q$  and  $\Delta H_{1/2}$  yields  $K_{ax} \approx -0.05\%$  for both crystallographic sites. The accuracy of this estimate is insufficient to allow a determination of possible temperature dependences in the shift anisotropy. Because of the small magnitude of  $K_{ax}$ , the shifts in Table I are essentially equal to  $K_{iso}$ .

### B. Nuclear-Spin Relaxation Rates

An accurate experimental determination of the spin-lattice relaxation rates in dhcp lanthanum is difficult to achieve. For example, complete saturation of the nuclear resonances is made difficult by the large quadrupole splittings. Partial saturation leads to a recovery behavior which can be described by a sum of several exponential terms.<sup>19-21</sup> For the case of magnetic-hyperfine relaxation processes and  $I = \frac{7}{2}$  these are characterized by the four time constants  $(1/28)T_1$ ,  $(1/15)T_1$ ,  $(1/6)T_1$ ,  $T_1$ , and amplitudes which depend on the initial populations of the  $2I+1$  spin levels. The early time dependence is, of course, dominated by the fastest rate which in the present case is  $28T_1^{-1}$ . Although the recovery of the longitudinal magnetization always tends asymptotically toward the intrinsic rate  $T_1^{-1}$ , this limiting rate is usually masked by noise or instrumental instabilities unless the fast relaxation components are strongly suppressed. In the present case, this was accomplished by using saturating combs composed of a large number of narrow rf pulses at the central-

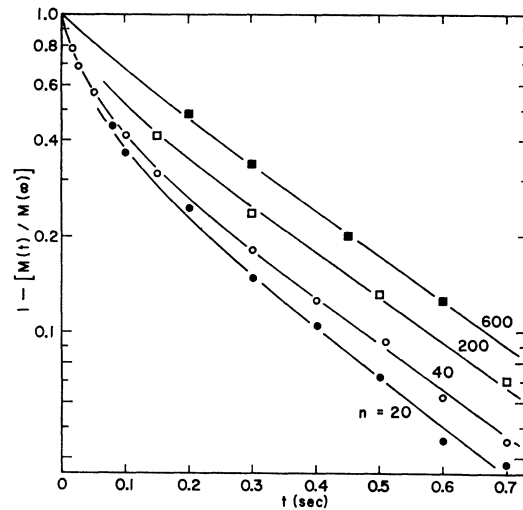


Fig. 4. Recovery of the longitudinal nuclear magnetization in dhcp lanthanum metal at 12 MHz and  $T = 1.95^\circ\text{K}$  following a saturating comb (0.5-sec duration) composed of  $n$  equally spaced  $3\text{-}\mu\text{sec}$ -wide rf pulses.

transition frequency. This is illustrated by the 12 MHz recovery curves in Fig. 4 which were obtained at  $1.95^\circ\text{K}$ . Because of the low frequency and the narrow ( $3\text{-}\mu\text{sec}$ ) rf pulses, this experiment did not discriminate between the two sites, i.e., both central transitions contributed equally to the observed echo amplitudes. The relaxation process following a comb of 600 pulses is nearly exponential with a relaxation time [defined as the point at which the signal amplitude has recovered to a value of  $(1-e^{-1})M_0$ , where  $M_0$  is the thermal equilibrium amplitude] of 0.29 sec. Experiments at other temperatures in the range  $T = 1\text{--}4^\circ\text{K}$  established that this relaxation time varies as  $T^{-1}$  with

$$T_1 T = 0.56(5) \text{ sec } ^\circ\text{K}. \quad (3.6)$$

The much smaller value of  $0.05 \text{ sec } ^\circ\text{K}$  reported by Masuda<sup>12</sup> can probably be attributed to incomplete saturation effects as illustrated by the recovery curves in Fig. 4 for small numbers of saturating rf pulses. The small deviation from a simple exponential time dependence even for the 600 pulse comb in Fig. 4 is indicative of either residual incomplete saturation or, more likely, slightly different relaxation rates for the two nonequivalent sites. In fact, the naive assumption  $T_1^{-1} \propto K^2$  leads to a predicted ratio of  $\sim 2.8$  for the two relaxation rates. In order to establish the actual ratio of the relaxation times, experiments were carried out near 30 MHz in which the initial recovery rates of the two central transitions were measured separately. This was accomplished by the use of a small number of saturating pulses having sufficient widths to limit saturation to a narrow spectral region. The optimum pulse parameters were determined by applying the saturating comb at one of the central-transition frequencies and measuring the signal amplitude immedi-

<sup>18</sup> R. G. Barnes, F. Borsa, S. L. Segel, and D. R. Torgeson, Phys. Rev. **137**, A1828 (1965).

<sup>19</sup> E. R. Andrew and D. P. Turnstall, Proc. Phys. Soc. (London) **78**, 1 (1961).

<sup>20</sup> W. W. Simmons, W. J. O'Sullivan, and W. A. Robinson, Phys. Rev. **127**, 1168 (1962).

<sup>21</sup> A. Narath, Phys. Rev. **162**, 320 (1967).

ately following the comb as a function of frequency by means of a second pulsed rf signal source. The comb duration and pulse widths were then adjusted to yield a sharply defined region of saturation covering the width of the central transition. In the actual relaxation experiments, the magnetic field was slowly swept through the central-transition region and the spin-echo spectrum for a given time delay from the saturating comb was recorded. The central-transition intensities were then obtained from the observed difference between the peak heights of the spectrum and the satellite background intensity (which recovers at a slightly different initial rate). Examples of experimental recovery data obtained under these conditions at 4°K are shown in Fig. 5. The effective relaxation times  $T_{1,eff}$  are quite short, as expected. If only the  $m = +\frac{1}{2}$  and  $m = -\frac{1}{2}$  populations were affected by the saturating comb, the initial rate constant would be given by  $28 T_1^{-1}$  as noted above. Applying this factor to the measured effective relaxation times of 7.1 and 4.1 msec yields  $T_1(1) = 0.19$  sec and  $T_1(2) = 0.11$  sec, respectively, where  $T_1(1)$  refers to the site having the smaller Knight shift while  $T_1(2)$  refers to the site having the larger of the two shifts. The average value of the two relaxation rates corresponds to  $T_1 T = 0.58$  sec °K which is in good agreement with the value given by (3.6). Although the slopes of the individual recovery curves varied somewhat from one experiment to the next, depending on the details of the saturating comb parameters, the ratio of the slopes was quite reproducible. An average of all of our 4°K results yields

$$T_1(1)/T_1(2) = 1.7(2). \quad (3.7)$$

Similar experiments at 27°K gave the same value. It is, of course, difficult to verify the absolute accuracy of these results. Some uncertainty, for example, is introduced by the subtraction of the satellite background. Spin-diffusion effects may also not be entirely negligible. Nevertheless, we believe that the ratio given

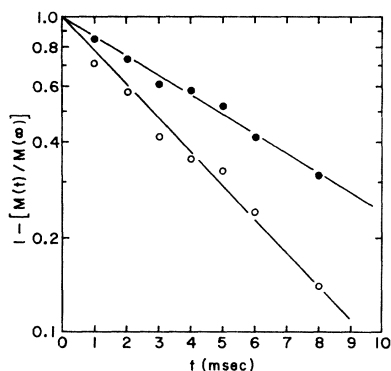


FIG. 5. Recovery of the central-transition spin-echo intensities at 30 MHz and 4.0°K following saturation by a 2-msec-duration comb composed of 21 20- $\mu$ sec-wide rf pulses. Open circles indicate low-field central peak. Filled circles indicate high-field central peak.

in (3.7) is reliable within the indicated uncertainty limits.

Because of the relatively small difference between  $T_1(1)$  and  $T_1(2)$ , the individual spin-lattice relaxation rates may be estimated by combining (3.6) and (3.7) according to  $T_1^{-1} \approx \frac{1}{2}[T_1(1)^{-1} + T_1(2)^{-1}]$ . We find  $T_1(1)T \approx 0.76$  sec °K and  $T_1(2)T \approx 0.44$  sec °K.

No detailed measurements of the spin-echo phase-memory times were attempted. In general, the observed  $T_2$  values ranged between 300 and 800  $\mu$ sec depending on the experimental conditions.

## IV. DISCUSSION

### A. Electric Field Gradients

The present value of  $\nu_Q$  for dhcp lanthanum is equivalent to a quadrupole coupling constant  $|e^2qQh^{-1}| = 7.8(3)$  MHz. (The sign of the coupling constant cannot be determined from our experimental results.) Using  $Q^{(139)} = 0.21 \times 10^{-24}$  cm<sup>2</sup> leads to an electric field gradient (EFG) whose magnitude is consistent with that obtained by Barnes *et al.*<sup>18</sup> for hcp scandium metal. This conclusion is based on calculations of the respective field gradients using the point-ion model. In this model the ion cores are treated as positive point charges, while the conduction electrons are assumed to form a uniform background of negative charge. The resulting lattice EFG ( $q_{latt}$ ) is corrected by a factor  $(1 - \gamma_\infty)$  for antishielding effects arising from the core electrons in the central cell, where  $\gamma_\infty$  is the Sternheimer antishielding factor.<sup>22</sup> It is generally recognized that the point-ion model provides at best a crude description of the actual charge distribution, particularly in transition metals where the  $d$  electrons are strongly localized. The model may nevertheless provide meaningful ratios for the field gradients of isoelectronic metals such as lanthanum and scandium since the respective conduction-electron contributions to the EFG are expected to scale linearly in that case with the lattice EFG. The  $A$ -site EFG in dhcp lanthanum is identical to the EFG in an hcp lattice having an equivalent  $c/a$  ratio. This follows from the fact that the  $B$ - and  $C$ -site sublattices are related to each other by inversion through the  $A$  sites, and therefore make identical contributions to the  $A$ -site EFG. The lattice sums required for an evaluation of the hcp EFG have been calculated by deWette<sup>23</sup> as a function of  $c/a$  ratio using his plane-wise summation method. The calculated and experimental EFG's are compared in Table II. The calculated values are based on an assumed point-ion charge  $Z = +3$ , and Sternheimer factors of  $-7$  and  $-73$  for scandium<sup>18</sup> and lanthanum,<sup>14</sup> respectively. The lattice constants were taken to be  $a = 3.309$  Å and  $c/a = 1.5936$  for hcp scandium<sup>24</sup> and  $a = 3.770$  Å

<sup>22</sup> R. Sternheimer, Phys. Rev. **84**, 244 (1951).

<sup>23</sup> F. W. deWette, Phys. Rev. **123**, 103 (1961).

<sup>24</sup> F. H. Spedding and A. H. Daane, J. Metals **6**, 504 (1954).

TABLE II. Comparison of experimental and point-ion electric field gradients (in units of  $10^{-22}$  cm $^{-3}$ ) for the hexagonal lattice sites in scandium and lanthanum. The experimental values were obtained from the measured quadrupole coupling constants using  $|Q^{(139)}| = 0.21 \times 10^{-24}$  cm $^2$  and  $|Q^{(45)}| = 0.22 \times 10^{-24}$  cm $^2$ . The calculated values are based on ionic charges, lattice constants, and Sternheimer antishielding factors given in the text.

	Scandium*	Lanthanum
$ q_{\text{expt}} $	$26.4 \pm 0.4$	$106 \pm 4$
$ q_{\text{latt}} (1 - \gamma_{\infty})$	11.3	40

\* Reference 18.

and  $c/a = 3.2252$  for dhcp lanthanum.<sup>9</sup> Although the agreement between the individual calculated and experimental EFG's is not good, the relative magnitudes for the two metals are in good agreement with experiment. This conclusion rests on the assumption, of course, that the sign of the EFG's are the same for both metals.

The point-ion model can also account for the observation of essentially identical EFG's for the two nonequivalent sites in dhcp lanthanum. The calculated *B*- and *C*-site EFG is found to be only  $\sim 10\%$  smaller<sup>14,25</sup> than the *A*-site EFG. It should be noted that nearest and next-nearest neighbors contribute to the *B*- and *C*-site EFG because the lanthanum  $c/a$  ratio deviates from its ideal value, thus causing a slight distortion in the cubic near-neighbor environment of these lattice sites. The small magnitude of the EFG at the hexagonal *A* sites is associated with the fact that the EFG for the hcp lattice reverses sign for  $c/a \sim 1.634$ .

It appears that the conduction electrons make a significant contribution to the observed quadrupole coupling constants in scandium and lanthanum. The magnitude of this contribution cannot be determined reliably, however, because of the unknown signs of the EFG as well as uncertainties in the magnitudes of the Sternheimer factor.

### B. Magnetic-Hyperfine Interactions

The important hyperfine coupling mechanisms in transition metals are associated with *s*-contact, *d*-core-polarization, and *d*-orbital interactions. For cubic crystals, and in the absence of significant spin-orbit effects, each of these mechanisms contributes independently to the Knight shift and spin-lattice relaxation rate.<sup>26-28</sup> The individual contributions can be represented for an independent-electron tight-binding model by

$$K_i = (\mu_B N)^{-1} H_{\text{hfs}}^{(i)} \chi_i, \quad (4.1)$$

$$R_i = (4\pi/\hbar) (\gamma_n \hbar)^2 k_B [H_{\text{hfs}}^{(i)} N_i(0)]^2 F_i, \quad (4.2)$$

<sup>25</sup> Using deWette's (Ref. 23) plane-wise summation technique, Torgeson and Barnes (Ref. 14) have obtained  $q_{\text{latt}} = 0.487 \times 10^{22}$  cm $^{-3}$  for the cubic site; using a direct summation technique, we find  $q_{\text{latt}} = 0.51 \times 10^{22}$  cm $^{-3}$ . These values should be compared with the hexagonal-site value  $q_{\text{latt}} = 0.542 \times 10^{22}$  cm $^{-3}$ .

<sup>26</sup> J. Korryng, *Physica* **16**, 601 (1950).

<sup>27</sup> Y. Yafet and V. Jaccarino, *Phys. Rev.* **133**, A1630 (1964).

<sup>28</sup> Y. Obata, *J. Phys. Soc. Japan* **13**, 1020 (1963).

where  $R \equiv (T_1 T)^{-1}$ ,  $N$  is Avogadro's number,  $H_{\text{hfs}}^{(i)}$  are appropriate hyperfine fields (per Bohr magneton),  $\chi_i$  are electronic susceptibilities,  $N_i(0)$  the *s*- and *d*-bare-electron state densities at the Fermi level for one direction of the spin as appropriate,  $F_i$  are inhibition factors which arise from the orbital degeneracy of the *d* bands (and thus apply only to the *d*-hyperfine rates, i.e.,  $F_s = 1$ ), and the remaining symbols have their usual meaning. It is obvious that a quantitative interpretation of transition-metal hyperfine effects requires a knowledge of many interaction parameters. In the case of the Group-IIIB transition metals, the analysis is further complicated by the hexagonal structure which makes it more difficult to estimate the *d*-relaxation inhibition factors.<sup>21</sup> The lower symmetry also leads to interference effects between the *s*-contact and *d*-core-polarization relaxation processes, as well as to an anisotropic orbital relaxation rate, unless the five *d* functions have equal weights in the conduction-electron wave functions at the Fermi level.<sup>21</sup> Finally, an accurate treatment of the relaxation rates must take account of enhancement effects resulting from electron-electron interactions.<sup>29,30</sup>

The electronic properties of the Group-IIIB transition metals are at present not sufficiently well understood to make a detailed analysis of the lanthanum Knight shifts and spin-lattice relaxation rates very meaningful. For this reason we will base our discussion on a comparison of the lanthanum data with previous results<sup>18,31,32</sup> for scandium and yttrium. A useful starting point for such an analysis is the crude assumption that the Group-IIIB metals can be represented, as far as magnetic-hyperfine effects are concerned, by an independent-electron gas in which the *s*-contact interaction is the only significant coupling mechanism between the nuclear and conduction-electron spins. For this model, (4.1) and (4.2) yield the well-known Korringa relation<sup>26</sup>

$$K^2 T_1 T = S, \quad (4.3)$$

where

$$S \equiv (\gamma_e / \gamma_n)^2 (\hbar / 4\pi k_B). \quad (4.4)$$

There are several reasons for believing that the *s*-contact mechanism contributes significantly to the total hyperfine interaction in the Group-IIIB metals. In the first place, the experimental Knight shifts are positive and considerably larger than can be accounted for by orbital paramagnetism associated with the *d* bands. For example, Gardner and Penfold<sup>5</sup> have estimated that the orbital Knight shift in scandium accounts for only half of the measured shift. Additional

<sup>29</sup> T. Moriya, *J. Phys. Soc. Japan* **18**, 516 (1963).

<sup>30</sup> A. Narath and H. T. Weaver, *Phys. Rev.* **175**, 373 (1968).

<sup>31</sup> A. Narath and A. T. Fromhold, Jr., *Phys. Letters* **25A**, 49 (1967).

<sup>32</sup> The value  $T_1 T = 1.6(1)$  given in Ref. 31 was obtained for a scandium sample which was not annealed after comminution; vacuum annealing reduced the relaxation time to the value given in Table III. The lower value is in good agreement with independent measurements by J. Butterworth (private communication).

evidence for the importance of  $s$ -contact interactions is provided by the temperature dependence of the shifts. In both scandium and lanthanum the susceptibilities and Knight shifts decrease with increasing temperature (i.e.,  $dK/dX > 0$ ). It seems likely that most of the observed temperature dependence is associated with the spin susceptibility.<sup>5</sup> One must conclude, therefore, that the magnitude of  $K_s$  exceeds that of  $K_d$  (since  $K_s > 0$  while  $K_d < 0$ ), and that  $s$ - $d$  mixing is sufficiently strong that  $\chi_s/\chi_d$  remains approximately constant at all temperatures. The absence of independent  $s$  and  $d$  bands at the Fermi level is entirely consistent with results of recent augmented-plane-wave (APW) band-structure calculations for scandium.<sup>33</sup>

The experimental values of  $K^2T_1T$  are compared in Table III with the theoretical Korringa products as given by (4.4). The  $K^2T_1T/S$  ratios exceed unity in all three metals, the deviation being largest in the case of lanthanum. There are two probable sources for these discrepancies. The first is the exchange enhancement of the spin susceptibilities. Since the relative enhancement of  $\chi(\mathbf{q})$  usually decreases with increasing wave vector  $\mathbf{q}$ , the square of the Knight shift is expected to be enhanced by a larger factor than the relaxation rate. The resulting increase in the Korringa product amounts to  $\sim 60\%$  in the nearly free-electron alkali metals<sup>30</sup> where collective-electron effects enhance the uniform spin susceptibility by approximately the same amount. Allowing for an orbital susceptibility  $\chi_{VV} \approx 10^{-4}$  emu/mole,<sup>5,6</sup> the enhancement of the uniform spin susceptibility of scandium, based on a comparison of experimental<sup>4</sup> and band theory<sup>33</sup> derived susceptibilities, amounts to a factor of  $\sim 4$ . An enhancement factor of this magnitude is in principle more than sufficient to yield the observed values of  $K^2T_1T/S$ . However, there exists evidence that the exchange enhancement of  $\chi(\mathbf{q})$  in the Group-IIIB metals is not a monotonically decreasing function of  $\mathbf{q}$ .<sup>34</sup> Rather, it appears that the enhancement may be largest for a nonzero  $\mathbf{q}$ . The enhancement of the relaxation rate may therefore be anomalously large,<sup>35</sup> and that of  $K^2T_1T$  correspondingly small. (In fact, it is in principle possible for  $K^2T_1T$  to be depressed below its Korringa value.)

Deviations of the experimental  $K^2T_1T$  products from the simple Korringa prediction can, of course, also result from  $d$ -spin and  $d$ -orbital hyperfine interactions. Because of the quadratic dependence of the relaxation rate on the various interaction parameters, it is sufficient for the present purpose to ignore all non- $s$  contact contributions to  $T_1T$  and to include the effects of the

TABLE III. Summary of low-temperature ( $\sim 4^\circ\text{K}$ ) Knight-shift and spin-lattice relaxation data for the hexagonal Group-IIIB transition metals. The lanthanum data are averages for the two nonequivalent lattice sites.

	<sup>46</sup> Sc	<sup>89</sup> Y	<sup>139</sup> La
$K_{i\rightarrow o}$ (%)	$+0.28 \pm 0.01^{a,b}$	$+0.37 \pm 0.01^{b,c}$	$+0.83 \pm 0.04$
$T_1T$ (sec $^\circ\text{K}$ )	$1.3 \pm 0.2^{c,d}$	$15 \pm 2^c$	$0.56 \pm 0.05$
$K^2T_1T/S$	2.3	1.9	2.9

<sup>a</sup> Reference 11.  
<sup>b</sup> Reference 18.  
<sup>c</sup> Reference 31.  
<sup>d</sup> Reference 32.

$d$ -electron interactions only in  $K$ . It is clear that  $d$ -orbital contributions enhance the Korringa product while small  $d$ -spin core-polarization contributions decrease its magnitude. Well-known examples of the former effect are provided by molybdenum<sup>36</sup> and tungsten<sup>37</sup> whose  $K^2T_1T/S$  ratios are 18 and 27, respectively. The latter effect is observed in the transition metal oxide  $\text{ReO}_3$ <sup>38</sup> whose  $K^2T_1T/S$  ratio is less than unity because its conduction-band states are almost purely  $d$  like near the Fermi level. It follows that the enhanced values of the Group-IIIB Korringa products can be at least partially attributed to  $d$ -hyperfine interactions, provided only that  $K_{VV} > |K_d|$ . The relative importance of collective-electron and  $d$ -hyperfine effects on the Korringa products can unfortunately not be determined unambiguously from the available information. It is nevertheless interesting to note that the magnitude of  $K^2T_1T/S$  is greatest for lanthanum<sup>39</sup> where the exchange enhancement of the spin susceptibility is probably the smallest. It is possible that this behavior is associated with the proximity of the empty  $4f$  band to the Fermi level of lanthanum. Since the orbital hyperfine coupling constant of the  $4f$  states is larger than that of the  $5d$  states,<sup>40</sup> the orbital Knight shift in lanthanum may have an appreciable magnitude. In this connection it would be interesting to measure the Knight shift and spin-lattice relaxation rate of lutetium metal which, because of its filled  $4f$  shell, resembles scandium and yttrium more closely than does lanthanum.

Despite the many uncertainties inherent in the analysis presented above, the importance of the  $s$ -contact interaction in the Group-IIIB metals appears well established. In particular, it seems certain that the magnitude of the direct contact shift exceeds that of the core-polarization shift. For this reason the core-polarization contribution to the measured spin-lattice relaxation rates must be relatively unimportant. This

<sup>33</sup> G. S. Fleming and T. L. Loucks, Phys. Rev. **173**, 685 (1968).

<sup>34</sup> This conclusion is based on the observation of helical  $4f$  spin structures in scandium and yttrium containing rare-earth solutes (e.g., Tb, Ho, Er) [see, for example, H. R. Child and W. C. Koehler, Phys. Rev. **174**, 562 (1968)]. This behavior is believed to be associated with the accidental occurrence of relatively parallel, nested pieces of Fermi surface [Ref. 33; see also D. Wohleben, Phys. Rev. Letters **21**, 1343 (1968)].

<sup>35</sup> S. Doniach, J. Appl. Phys. **39**, 483 (1968).

<sup>36</sup> A. Narath and D. W. Alderman, Phys. Rev. **143**, 328 (1966).

<sup>37</sup> A. Narath and A. T. Fromhold, Jr., Phys. Rev. **139**, A794 (1965).

<sup>38</sup> A. Narath and D. C. Barham, Phys. Rev. **176**, 479 (1968).

<sup>39</sup> Strictly speaking, this statement applies to the site having the larger of the two Knight shifts. For this site  $K^2T_1T/S \approx 3.5$ .

<sup>40</sup> See, for example, A. J. Freeman and R. E. Watson, in *Magnetism*, edited by G. T. Rado and H. Suhl (Academic Press Inc., New York, 1965), Vol. 2A, Chap. 5.



also applies to the orbital relaxation since orbital hyperfine fields are in general no larger than core-polarization fields. In order to examine the implications of this conclusion we have calculated the  $d$ -hyperfine relaxation terms based on the following assumptions. The orbital hyperfine fields were calculated according to  $H_{\text{hfs}}^{\text{(orb)}} = 2\mu_B \langle r^{-3} \rangle$ , using estimated neutral atom  $\langle r^{-3} \rangle$  values.<sup>40</sup> For the core-polarization hyperfine fields the free-ion value was taken in the case of scandium,<sup>5</sup> while the core-polarization fields of metallic palladium<sup>41</sup> and platinum<sup>42</sup> were used for yttrium and lanthanum, respectively. The admixture coefficients of the five  $d$  states were assumed to be equal and the inhibition factors were therefore taken to be  $F_{\text{orb}} = 0.4$  and  $F_d = 0.2$ .<sup>21</sup> Finally,  $N_d(0)$  was initially set equal to the total density of states as calculated from the electronic specific heat<sup>2,3</sup> in the independent electron approximation. The resulting relaxation rates, as shown in Table IV, are faster than the experimental rates, rather than slower as required by our Knight-shift analysis. It must also be remembered that inclusion of exchange-enhancement effects would increase the calculated rates even more.

The discrepancies, which are particularly large for yttrium and lanthanum, can be attributed to two causes. Probably the more obvious of these is an overestimate of the bare-electron state densities. For example, band-structure calculations for scandium<sup>32</sup> and yttrium<sup>43</sup> have yielded values for  $N(0)$  which are only half as large as the specific-heat derived densities. This difference, which may in fact be even larger in the case of lanthanum, is undoubtedly for the most part due to electron-phonon interactions, although spin-fluctuation contributions may also be significant.<sup>44</sup> Another factor responsible for the excessively rapid relaxation rates calculated above is the choice of core-polarization hyperfine fields. The present results suggest that the strength of the core-polarization interaction may increase rapidly with increasing atomic number in the  $4d$  and  $5d$  transition periods, in contrast with the near constancy of  $3d$  core-polarization fields.<sup>40</sup> In other words, the palladium and platinum hyperfine fields may represent serious overestimates for yttrium and lanthanum, respectively. A further reduction in the core-polarization hyperfine fields in the Group-IIIB metals may result from positive  $4s$  contributions, as already noted by Gardner and Penfold.<sup>5</sup> That the net core-polarization field in lanthanum must be much smaller than in platinum can be seen most easily by comparing the Knight shifts in the two metals. The magnetic susceptibilities are almost identical. The Knight shift, however, is large and *negative* in platinum<sup>42</sup>

TABLE IV. Comparison of experimental spin-lattice relaxation rates (in units of  $10^{-8}$  Oe<sup>2</sup> sec °K<sup>-1</sup>) in the hexagonal Group-IIIB transition metals with calculated  $d$ -spin core-polarization and  $d$ -orbital rates. The calculated rates are based on hyperfine-field estimates (in units of  $10^6$  Oe/ $\mu_B$ ) and state densities (in units of  $10^{11}$  erg<sup>-1</sup> atom<sup>-1</sup>) shown in the table, and inhibition factors  $F_d = 0.2$  and  $F_{\text{orb}} = 0.4$ .

	<sup>45</sup> Sc	<sup>89</sup> Y	<sup>139</sup> La
$H_d$	-0.10	-0.36	-1.2
$H_{\text{orb}}$	+0.096	+0.14	+0.18
$N(0)\gamma$	14.9	13.5	13.4
$R_d/\gamma_n^2$	0.82	8.6	94
$R_{\text{orb}}/\gamma_n^2$	1.50	2.5	3.4
$(R_d + R_{\text{orb}})/\gamma_n^2$	2.3	11.1	97
$R_{\text{expt}}/\gamma_n^2$	1.8	3.9	12

and has a magnitude corresponding to  $K/\chi \approx -160$  (emu/mole)<sup>-1</sup>, while in lanthanum it is *positive* with  $K/\chi = +55$  (emu/mole)<sup>-1</sup>. In summary, it appears likely that realistic values for  $N(0)$  and  $H_{\text{hfs}}^{(d)}$  would bring the calculated  $d$ -hyperfine rates below the experimental rates.

Because of the large magnitude of  $s$ -contact hyperfine fields, only a relatively small  $s$  admixture at the Fermi level is required to yield shifts and relaxation rates comparable in magnitude to the observed values. Even allowing for a  $\sim 30\%$  reduction of the  $s$ -contact fields in the metals relative to their atomic values,<sup>45</sup> an  $s$ -electron susceptibility of  $\lesssim 20 \times 10^{-6}$  emu/mole is sufficient to account for the experimental results in all three Group-IIIB metals.

So far we have only considered the average values of the Knight-shift and spin-lattice relaxation rate in dhcp lanthanum. In view of the qualitative nature of the conclusions offered above, it is not possible to arrive at a unique interpretation of the large differences between the observed hyperfine effects at the two nonequivalent sites. It is interesting to note, however, that the two magnetic sublattices in the dhcp rare-earth metals neodymium and praseodymium exhibit different magnetic-ordering temperatures.<sup>46</sup> One may speculate that all of these characteristics are related to the same intrinsic difference (for example, the density-of-states function) in the local conduction-electron properties at the two sites in the dhcp structure.

## V. SUMMARY

The results of the present study show that the local conduction-electron properties at the two nonequivalent crystallographic sites in dhcp lanthanum metal are distinctly different. Although no differences in the electric field gradients were resolved, the Knight shifts and nuclear spin-lattice relaxation rates were found to differ significantly. The available information is not

<sup>41</sup> J. A. Seitchik, A. C. Gossard, and V. Jaccarino, Phys. Rev. **136**, A1119 (1964).

<sup>42</sup> A. M. Clogston, V. Jaccarino, and Y. Yafet, Phys. Rev. **134**, A650 (1964).

<sup>43</sup> T. L. Loucks, Phys. Rev. **144**, 504 (1966).

<sup>44</sup> M. A. Jensen and J. P. Maita, Phys. Rev. **149**, 409 (1966).

<sup>45</sup> D. A. Shirley and G. A. Westenbarger, Phys. Rev. **138**, A170 (1965).

<sup>46</sup> W. C. Koehler, J. Appl. Phys. **36**, 1078 (1965).

sufficient, however, to assign the observed hyperfine effects to specific lattice sites.

Because of the large number of presently unknown parameters, a detailed interpretation of the Knight shifts and spin-lattice relaxation rates in lanthanum, as well as the other two Group-IIIB transition metals, scandium and yttrium, is not possible at this time. Nevertheless, the data suggest strongly that the dominant magnetic-hyperfine mechanism in these metals is the direct *s*-contact interaction. It is also possible to conclude that the electron-phonon enhancement of the electronic specific heat is large, as indicated by the available band-structure calculations, and that the effective *d*-spin core-polarization hyperfine fields, at least in yttrium and lanthanum, are significantly smaller than in the corresponding Group-VIII metals, palladium and platinum.

As in the case of scandium, the lanthanum quadrupole coupling constant is approximately 2.5 times larger than can be accounted for by the point-ion model. Thus, the relative importance of conduction-

electron contributions to the EFG is approximately the same in both metals.

*Note added in proof.* F. Y. Fradin, Phys. Letters **28A**, 441 (1968), has recently determined the field-orientation dependence of the spin-lattice relaxation rate in a single-crystal specimen of scandium. An analysis of the observed anisotropy based on the extreme tight-binding model<sup>21</sup> led to the conclusion that the orbital hyperfine interaction is the dominant relaxation mechanism in scandium metal. Because of the many approximations inherent in the model the accuracy of this conclusion is difficult to assess.

#### ACKNOWLEDGMENTS

The author is indebted to Professor R. G. Barnes for his interest in this work as well as for the loan of his lanthanum sample. Several stimulating discussions with Dr. D. B. McWhan were most helpful. The author is especially grateful to D. C. Barham and Dr. H. T. Weaver for their expert experimental assistance.

### Quantum Theory of an Optical Maser. III. Theory of Photoelectron Counting Statistics\*

MARLAN O. SCULLY†

*Department of Physics and Materials Science Center, Massachusetts Institute of Technology, Cambridge, Massachusetts 02139*

AND

WILLIS E. LAMB, JR.‡

*Department of Physics, Yale University, New Haven, Connecticut 06520*

(Received 31 January 1968)

In this paper we determine the photoelectron counting statistics produced by the fully quantum-mechanical laser considered in the first paper of this series. The problem of obtaining the photocount distribution from the now known photon statistics is solved in a completely quantum-mechanical fashion. The time evolution of the combined photodetector-laser system is derived. The techniques developed for the solution of this problem are of general interest in the area of nonequilibrium quantum statistical dynamics.

#### I. INTRODUCTION

IN the first paper<sup>1</sup> of this series the steady-state photon distribution in a laser cavity (above, at, or below threshold) was found to be

$$\rho_{n,n} = Z^{-1} \left\{ \frac{(A^2/BC)^{n+A/B}}{(n+A/B)!} \right\}. \quad (1)$$

The photon statistical distribution is inferred in practice by photoelectron counting techniques. The photoelectron counting statistics produced by laser radiation

† Work supported by the Advanced Research Projects Agency under Contract No. SD-90.

‡ Work supported in part by the National Aeronautics and Space Administration and in part by the U. S. Air Force Office of Scientific Research.

<sup>1</sup> M. Scully and W. E. Lamb, Jr., Phys. Rev. **159**, 208 (1967). Symbols used in Eq. (1) are summarized in Sec. IV of the present paper.

\* A preliminary account of this work was presented at the Second Rochester Conference on Coherence and Quantum Optics.